

DETECTION OF THE $^3P_2 \rightarrow ^3P_1$ SUBMILLIMETER TRANSITION OF $^{13}\text{C I}$ IN THE INTERSTELLAR MEDIUM: IMPLICATION FOR CHEMICAL FRACTIONATIONJOCELYN KEENE,¹ PETER SCHILKE,² J. KOOL,¹ D. C. LIS,¹
DAVID M. MEHRINGER,¹ AND T. G. PHILLIPS¹*Astrophysical Journal Letters, in press*

ABSTRACT

We report the first detection of the submm emission from the ^{13}C isotope of atomic carbon in the ISM. The $F = 5/2 - 3/2$ component of the $^3P_2 - ^3P_1$ transition was observed with the CSO in a region $\sim 4'$ S of Orion IRc2, near the western end of the Orion Bar. The ^{12}C to ^{13}C isotopic abundance ratio is 58 ± 12 corrected for opacity of the $^{12}\text{C I}$ line and the fractional intensity of the $^{13}\text{C I}$ hyperfine component (60%). This is in agreement with the value for the equivalent ratio in C^+ . In comparison, our measurement of the C^{18}O to $^{13}\text{C}^{18}\text{O}$ ratio from observations of 2–1 and 3–2 lines toward the same position gives a value of 75 ± 9 . PDR models predict that the ^{12}C to ^{13}C abundance ratio is particularly sensitive to chemical fractionation effects. If $^{13}\text{C}^+$ is preferentially incorporated into ^{13}CO at cloud edges there will be a dramatic reduction in the abundance of ^{13}C . This is contrary to our observations, implying that the importance of chemical fractionation is small or is compensated for by isotopic-selective photo-dissociation of ^{13}CO in this region with a large UV illumination.

Subject headings: ISM: abundances — ISM: atoms — ISM: individual (Orion Molecular Cloud, Orion Bar) — ISM: molecules — radio lines: ISM

1. INTRODUCTION

The abundances and ratios of the CNO isotopes in the interstellar medium (ISM) are sensitive to details of stellar and Galactic chemical evolution. Many attempts have been made to measure the ratio of ^{12}C to ^{13}C throughout the Galaxy and in the local ISM, as well as in stars, to help guide the Galactic evolutionary models. Optical, UV, and IR absorption line techniques have been used for these measurements as well as radio emission line measurements (see the review by Wilson & Rood 1994).

One of the most successful attempts for ISM measurements has been made by Langer & Penzias (1990 & 1993; hereafter LP90 & LP93) who compared the weak emission lines of C^{18}O and $^{13}\text{C}^{18}\text{O}$. They found a Galactic gradient in the ^{12}C to ^{13}C ratio ranging from ~ 25 near the Galactic center to about 60 to 70 at a Galactic radius (R_G) of about 10 kpc. The value in the local ISM is 62 ± 4 . For $R_G > 16$ kpc, Wouterloot & Brand (1996), using the same technique, found a value > 100 . Ratios derived from observations of H_2CO show a similar Galactic gradient but are $\sim 50\%$ higher (Wilson & Rood 1994). Unfortunately, ratios derived from both CO and H_2CO can be distorted by chemical fractionation and isotopic-selective photo-dissociation, two processes discussed further in §4.

Centurión et al. (1995) have reviewed the various determinations using optical absorption lines of CH^+ and concluded that the abundance ratio in the local ISM is 67 ± 3 . Boreiko and Betz (1996) have measured the $^{12}\text{C}^+$ to $^{13}\text{C}^+$ ratio for the average of several positions toward the Orion Nebula region. The value they found is 58 ± 6 . It is thought that neither of these probes should suffer from chemical fractionation effects.

In this letter we describe measurements of the ratio with another fundamental probe, neutral atomic carbon. According to PDR models, the ratio of atomic ^{12}C to ^{13}C in the dense interstellar medium is particularly sensitive to the opposing effects of chemical fractionation and isotopic-selective photo-dissociation which can also affect the isotopomeric ratios of many molecules, e.g., CO and H_2CO . In this paper we use the atomic carbon isotopic ratio to assess the relative importance of these effects in one astronomical source. We compare the isotopic ratio in atomic carbon to that in CO, through measurements of the weak lines of $^{13}\text{C}^{18}\text{O}$ and C^{18}O which are similarly affected by chemical fractionation and isotopic-selective photo-dissociation as the more abundant species (Langer et al. 1984; van Dishoeck & Black 1988).

¹Caltech Submillimeter Observatory, Caltech 320-47, Pasadena, CA 91125; jbk,kool,dcl,mehring,phillips@tacos.caltech.edu

²Max-Planck-Institut für Radioastronomie, Auf dem Hügel 69, 53121 Bonn, Germany; schilke@mpifr-bonn.mpg.de

The $^3P_1 - ^3P_0$ transition of ^{12}C I at 492 GHz has been available for high spectral resolution measurements in molecular clouds for many years. Unfortunately, the equivalent ^{13}C I transition is insufficiently split from the ^{12}C I line to allow its discrimination; the largest split is only 3.6 MHz (2.2 km s^{-1} ; Yamamoto & Saito 1991). However, the splitting between the ^{12}C I ($^3P_2 - ^3P_1$) and the strongest hyperfine component of the ^{13}C I equivalent transition, both lying near 809 GHz, is 152 MHz (56 km s^{-1} ; Klein et al. 1997), providing a better opportunity for detection of ^{13}C I.

2. OBSERVATIONS

The observations were made during two periods of good weather in 1996 December and 1997 February with the recently available 850 GHz receiver (Kooi et al. 1997) at the Caltech Submillimeter Observatory (CSO). The 225 GHz zenith opacity at the time was ~ 0.03 , corresponding to an 809 GHz opacity of ~ 0.7 . We observed ^{12}C I and ^{13}C I in the upper sideband in 1996 December and in the lower sideband in 1997 February. There was excellent agreement between the two observing runs. Using Mars (diameter $10''.6$), we measured the main beam efficiency at 809 GHz to be 33% in 1997 February assuming the theoretical beamsize of $9''$. Our source is very extended, so the Moon efficiency would be more appropriate to use in correcting the measured intensities. We estimate it to be $60\% \pm 20\%$. In addition we measured some of the lines of CO and its isotopomers in the 2–1 and 3–2 transitions.

We decided to observe the $F = 5/2 - 3/2$ component of the $^3P_2 - ^3P_1$ transition of ^{13}C I because it is the strongest of the three components, with 60% of the total line-strength. We centered this component within the quietest part of our bandpass which meant that the two weaker components were not observed.

We chose to observe a position in the clump at the base of the Orion Bar ionization front, $\alpha(1950) = 5^{\text{h}}32^{\text{m}}47^{\text{s}}.7$, $\delta(1950) = -5^{\circ}28'30''$, ($\sim 4'$ S of IRC2) because it is known to have bright 492 GHz C I lines (Tauber et al. 1995). Unlike the Bar itself, the clump does not appear to have a strong edge-on geometry. It also has a simple molecular spectrum, thus avoiding line confusion such as occurs near Orion IRC2.

The fine-structure energy level intervals of the ^{12}C and ^{13}C atoms have been measured with high precision in the laboratory by Saykally & Evenson (1980), Cooksy et al. (1986), Yamamoto & Saito (1991), and most recently by Klein et al. (1997, Letter this issue).

3. RESULTS

The observed spectra of ^{13}C I and ^{12}C I and the comparison isotopomeric lines of CO are shown in

Figure 1. This is the first detection of submillimeter emission from ^{13}C in the ISM. We measured the frequency of the ^{12}C I and ^{13}C I lines by comparison with the ^{13}CO (2–1) line (not shown) which has a shape nearly identical to that of the ^{12}C I line. The frequency we measure for the $^3P_2 - ^3P_1$ transition of ^{12}C I is 809342.3 ± 0.4 MHz and the frequency of the $F = 5/2 - 3/2$ component of the $^3P_2 - ^3P_1$ transition of ^{13}C I is 809492.8 ± 1.1 MHz. These agree well with the new laboratory measurements by Klein et al. (1997).

To compare the atomic isotopic ratio to the molecular isotopomeric ratio we need to derive the ratio of column densities from the ratio of line intensities for both sets of data.

3.1. Atomic Carbon Isotopic Ratio

The column density ratio is derived from the line intensity ratio as follows:

$$\frac{N(^{12}\text{C})}{N(^{13}\text{C})} = \frac{S(^{13}\text{C})}{\beta(^{12}\text{C})} \frac{I(^{12}\text{C})}{I(^{13}\text{C})},$$

where N indicates column density, I is the measured integrated line intensity (in K km s^{-1}), S is the fractional strength of the $F = 5/2 - 3/2$ component of the $^3P_2 - ^3P_1$ transition of ^{13}C I, and $\beta = (1 - e^{-\tau})/\tau$ is the escape probability of the ^{12}C I line photons, which compensates for the finite optical depth, τ , in the ^{12}C I line.

Because of the low signal-to-noise ratio of the weak ^{13}C I line, we use three methods of measuring line intensity ratios. First, we integrate the line intensities over the interval 5 to 14 km s^{-1} . This method has the disadvantage of including excess noise outside the line core. Next, we integrate over the ^{13}C I and ^{12}C I line profiles weighted by the ^{12}C I line profile, a method used by LP90 for CO isotopomers to lessen the contribution of noise outside the line core. Finally, we fit Gaussians to the ^{12}C I line and use the same width and central velocities for the ^{13}C I line. The dispersion in these determinations is low (4%) and we adopt the mean value, 80. The S/N in the line integral measurement for the ^{13}C I line estimated from the noise in the baseline is ~ 6.5 so we assign a 15% uncertainty to the ratio. Thus the measured line intensity ratio is 80 ± 12 . Because the ^{13}C I and ^{12}C I lines were measured simultaneously in the same receiver sideband, there is no significant calibration uncertainty in the line intensity ratio.

The ^{13}C I transition has 3 hyperfine components. We assume that the excitation is thermal so that the hyperfine line intensities are proportional to the quantum mechanical line strengths and $S(^{13}\text{C}) = 0.6$.

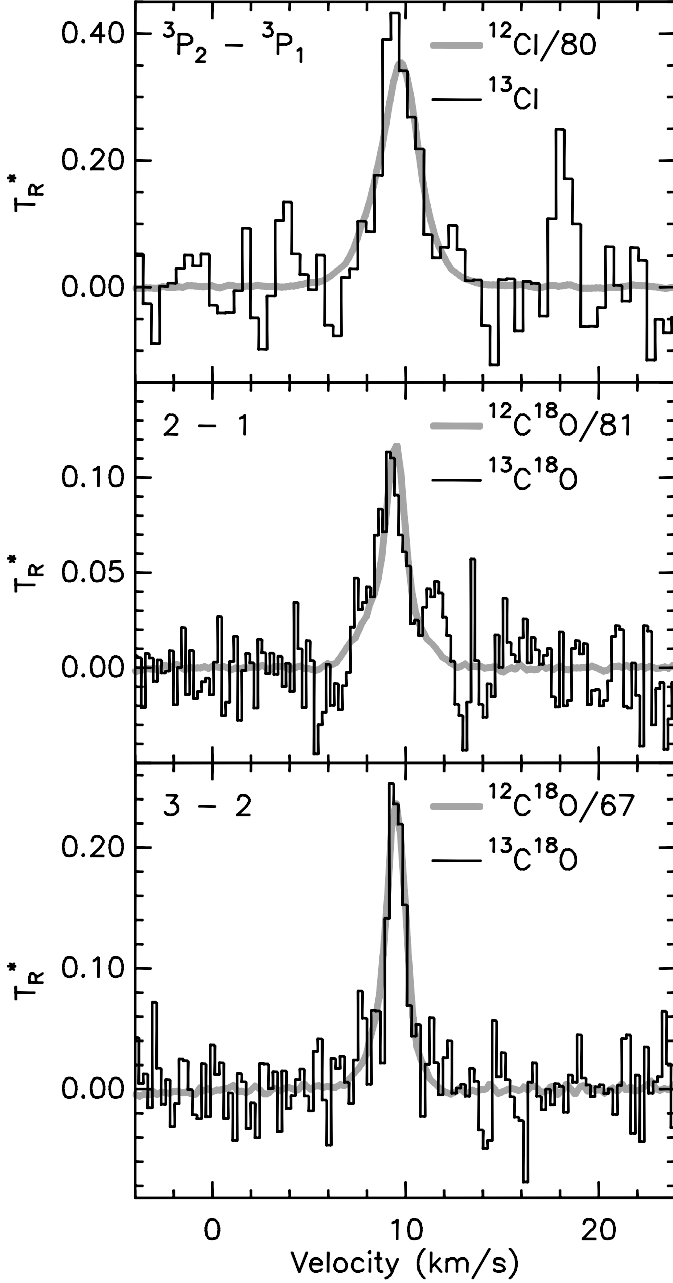


FIG. 1.— Observed spectra of (top) the $^3P_2 - ^3P_1$ transitions of $^{12}\text{C I}$ and $^{13}\text{C I}$ ($F = \frac{5}{2} - \frac{3}{2}$); (middle) the 2–1 transitions of $^{12}\text{C}^{18}\text{O}$ and $^{13}\text{C}^{18}\text{O}$; (bottom) the 3–2 transitions of $^{12}\text{C}^{18}\text{O}$ and $^{13}\text{C}^{18}\text{O}$. All spectra have been corrected for the estimated Moon efficiencies, 60% for C I and 70% for CO. The spectra of the species containing ^{12}C have been additionally scaled as indicated. In creating the velocity scales for these plots the frequencies for the CO isotopomers have been taken from Winniewisser, Winniewisser, & Winniewisser (1985).

The most difficult factor to estimate is the correction for the finite optical depth of the $^{12}\text{C I}$ line. We assume that the C I excitation temperature is 104 K, as we measured for the ^{12}CO (2–1) line, and that the telescope beam efficiency for large sources is

$60\% \pm 20\%$. The uncorrected line intensity of 17 K then corresponds to a true line intensity of 28.3^{+14}_{-7} K and an opacity $\tau = 0.40^{+0.28}_{-0.12}$ with line escape probability $\beta = 0.83^{+0.11}_{-0.04}$.

The resulting ratio of the ^{12}C to ^{13}C column densities is 58 ± 12 , where we have added the uncertainty in the escape probability in quadrature with that of the line intensity ratio.

3.2. CO Isotopomeric Ratios

The CO isotopomeric column density ratio is derived from the line intensity ratio as follows:

$$\frac{N(\text{C}^{18}\text{O})}{N(^{13}\text{C}^{18}\text{O})} = \frac{F}{\beta(\text{C}^{18}\text{O})} \frac{I(\text{C}^{18}\text{O})}{I(^{13}\text{C}^{18}\text{O})},$$

where F is a small correction due to the difference in the molecular excitation and the transition probabilities caused by the difference in frequency between the two lines.

We use the same three methods described in §3.1 for determining line intensity ratios and adopt the mean values of these determinations: 81 for the 2–1 lines and 67 for 3–2. Because the $^{13}\text{C}^{18}\text{O}$ lines are very weak, the uncertainties in the line ratios are substantial. One measure of the uncertainties is the ranges in the ratios determined by the three different methods. These are $\sim 7\%$ for the 2–1 ratio and $\sim 12\%$ for 3–2. The uncertainties in the integrated line intensities for the $^{13}\text{C}^{18}\text{O}$ 2–1 and 3–2 lines, as estimated from the noise in the baselines, are 10% and 9% respectively. To be conservative we adopt the larger of the two uncertainty estimates. We have estimated the telescope efficiency to be 70% for both 2–1 and 3–2 transitions based on past determinations. Because the frequencies of the two lines in each frequency range are so close, this should add little uncertainty to the ratios. A larger factor is the uncertainty in the sideband ratio, since we have double sideband receivers. We estimate this uncertainty to be 10% for each measurement or 14% for the ratio. Added in quadrature to the previous uncertainties, we have 17% uncertainty for the 2–1 line intensity ratio and 19% for 3–2.

Using standard LTE column density formulas we find for both the 2–1 and 3–2 lines that $F = 0.92$. We can also estimate this correction factor using an LVG calculation. Then we find $F = 0.91$ for 2–1 and $F = 0.94$ for 3–2, so uncertainty in determination of F is small and can be neglected.

We have estimated the optical depth of the C^{18}O lines using an LVG model for the C^{18}O (2–1) and (3–2) line intensities and ratio. The temperature and density are both constrained on the low ends by the line ratio which gives $T > 70$ K and $n(\text{H}_2) > 1.6 \times 10^4 \text{ cm}^{-3}$. We adopt the best fit for the temperature

given by the brightness temperature of the CO (2–1) line ($T = 104$ K, $n(\text{H}_2) = 3 \times 10^4 \text{ cm}^{-3}$) which has opacities of 0.09 and 0.27 and escape probabilities of 0.96 and 0.88 for the 2–1 and 3–2 lines respectively. These lie near the center of the possible range as derived from the LVG model. As a measure of the uncertainties we use the ranges of the escape probabilities, determined by the LVG calculation with different densities and temperatures. We find an uncertainty of $\sim 3\%$ for the 2–1 lines and $\sim 9\%$ for the 3–2 lines. The total uncertainty for $N(\text{C}^{18}\text{O})/N(^{13}\text{C}^{18}\text{O})$ is $\sim 17\%$ for the 2–1 line and $\sim 21\%$ for the 3–2 line.

Finally, combining all the factors, we find that $N(\text{C}^{18}\text{O})/N(^{13}\text{C}^{18}\text{O}) = 77 \pm 12$ from the 2–1 lines and 72 ± 15 from 3–2, with a weighted average of 75 ± 9 . In comparison, values of the ^{12}C to ^{13}C ratio toward the Orion Molecular Cloud previously derived from observations of C^{18}O and $^{13}\text{C}^{18}\text{O}$ (2–1) and (1–0) range from 79 ± 7 near IRC2 (LP90) to 63 ± 6 at a position $\sim 14'$ S of IRC2 (LP93). Our value lies within this range and closer to the IRC2 value as befits its position close to the H II region. The average for the solar neighborhood is 62 ± 2 (LP93), so the positions near the M42 H II region in Orion appear to be truly different from the average neighborhood value, possibly due to the strong UV field of the Trapezium.

4. DISCUSSION

As mentioned in §1 there are two major physical phenomena which can modify the abundance ratios of the various atomic and molecular forms of carbon and its isotopes. The first is chemical fractionation of ^{13}CO and ^{12}CO , due to the rapid exothermic exchange of $^{13}\text{C}^+$ with ^{12}C in CO preferentially forming ^{13}CO (Watson, Anicich & Huntress 1976). Since ^{13}C is formed by the recombination of $^{13}\text{C}^+$, ^{13}C will be depleted in favor of ^{13}CO . This process is most effective where there is a large abundance of C^+ ions and where the temperature is low, i.e., in the transition zone between ionized and molecular forms of carbon near the edges of molecular clouds. Here ionized, atomic and molecular forms of carbon co-exist and the temperature is reduced due to the enhanced cooling by atomic and molecular species. However, if the temperature were high the rapid ion exchange would push the ^{12}CO to ^{13}CO ratio toward the elemental ratio.

The second process is the isotopic-selective photo-dissociation of CO. Again, this is generally most effective near the edges of molecular clouds. It occurs because CO and its isotopes are partially self-shielding, in that the photo-dissociation of CO occurs through discrete lines in the ultraviolet. H_2 molecules and dust act to partially shield CO — H_2 through its heavily saturation-broadened UV absorption lines

and dust through continuum UV absorption. ^{12}CO is also very effective at shielding itself, because of its large abundance, but ^{13}CO is much less so, resulting in a greater photo-dissociation rate for ^{13}CO and enhancement of ^{13}C and $^{13}\text{C}^+$ abundances at the expense of ^{13}CO . The situation for photo-dissociation of C^{18}O and $^{13}\text{C}^{18}\text{O}$ seems to be similar, although the overall rates are higher for the less abundant species (van Dishoeck & Black 1988).

We have used the photo-dissociation region (PDR) model of Le Bourlot et al. (1993) to interpret our observations. This model incorporates both chemical fractionation and isotopic-selective photo-dissociation and we have used full radiative transfer, explicitly computing the mutual- and self-shielding of H_2 and all the CO isotopomers. We ran this model for a cloud of constant density $n(\text{H}_2) = 2.5 \times 10^4 \text{ cm}^{-3}$ with impinging UV field of strength $G_0 = 4 \times 10^4$ (Tauber et al. 1994) and abundances from Flower et al (1995). The total gas phase isotopic abundance ratios were taken to be $^{12}\text{C}/^{13}\text{C} = 60$ and $^{16}\text{O}/^{18}\text{O} = 500$. The results are shown in Figure 2.

Figures 2a & b show abundances and column densities of the majority carbon species as a function of extinction in the model cloud. Figures 2c & d show the abundance and column density ratios of the ^{12}C bearing species to their respective ^{13}C bearing species, normalized by their input ratios. Although most of the variation in the isotope ratios in 2c takes place at visual extinctions between about 2 and 7, we have observed a region of high column density, $A_V > 50$ as estimated from the C^{18}O column density marked in 2b ($2.5 \times 10^{16} \text{ cm}^{-2}$), so that these surface effects are seen integrated with the cloud interior, as shown in 2d and are thus, except for the atomic ^{12}C to ^{13}C ratio, greatly diluted.

An important feature of the model is that at extinctions between about 2 and 7 both ^{13}CO and $^{13}\text{C}^{18}\text{O}$ are enhanced through chemical fractionation relative to their ^{12}C isotopomers by factors up to 2.5 (Fig. 2c). The double ratio $n(^{12}\text{C}^{18}\text{O})/n(^{13}\text{C}^{16}\text{O})$ displays much more extreme behavior. This ratio is affected in the same sense by both chemical fractionation and isotopic-selective photo-dissociation. The first increases the abundance of ^{13}CO while the second decreases the abundance of C^{18}O . The result is that ^{13}CO is enhanced relative to C^{18}O by a factor up to 20 in the same range of extinction.

Another important feature is that the local abundance ratio of $n(^{12}\text{C})/n(^{13}\text{C})$ closely follows that found in C^+ (Fig 2c). These ratios vary in the opposite sense to the ratios found in CO. In this model, *where the temperature is low in the PDR (~ 25 K), chemical fractionation dominates over isotopic-*

selective photo-dissociation so that ^{13}C is underabundant in both atomic carbon and C^+ but is overabundant in CO.

Finally, although the *local abundance ratios* of C and C^+ track each other very well (Fig. 2c), there is no effect due to the PDR visible in the *column density ratio in C^+* (Fig. 2d), because C^+ is most abundant outside the molecular cloud where it is a majority species and where this effect is negligible. Therefore, according to this model, *the isotopic column density ratio measured in C^+ should give the true isotopic gas phase abundance ratio*. Boreiko and Betz (1996) have measured the $^{12}\text{C}^+$ to $^{13}\text{C}^+$ ratio for the average of several positions in the Orion Nebula region. The value they find for the ratio is 58 ± 6 . In contrast, *atomic carbon is most abundant in the model where the isotopic fractionation effects are most important*. Therefore there should be a large effect on the isotopic column density ratio of atomic carbon, as seen in the model (Fig. 2d). Yet the value we measure for the ^{12}C to ^{13}C ratio is 58 ± 12 , the same as the ratio in C^+ .

Our model in Figure 2d does not provide a good match to the observations indicated. The observed ratio of ^{12}C to ^{13}C is the same as the intrinsic ratio measured in C^+ by Boreiko & Betz (1996) and is lower than that in CO as measured using the rare isotopomeric species. The deviation is in the sense that this model evidently has a great deal too much chemical fractionation, which pushes the model ratio of ^{12}C to ^{13}C to a larger value than is consistent with our observations.

We were able to achieve better agreement between our data and the model by artificially increasing the temperature within the model cloud. This higher temperature suppresses chemical fractionation within the PDR. That such a high temperature (~ 120 K) may be present is indicated from observations of ^{13}CO (6–5) toward the Orion Bar (Lis, Schilke & Keene 1997) but how it can be achieved physically is beyond the scope of this Letter to discuss.

In summary, we have measured the ^{12}C to ^{13}C ratio in atomic carbon (58 ± 12) and find it to be the same as that in ionized carbon (58 ± 6 ; Boreiko & Betz 1996) and probably smaller than that found in C^{18}O (75 ± 9). The ratio of $^{12}\text{C}^+$ to $^{13}\text{C}^+$ should indicate the intrinsic isotopic abundance ratio since this is a majority species outside molecular clouds and it should not be significantly influenced by chemical fractionation or isotopic-selective photo-dissociation at cloud edges. From the PDR model, we see that the agreement between the isotopic ratios in ionized and atomic carbon implies that in this highly illuminated region chemical fractionation must be unimportant or is compensated for by isotopic-selective

photo-dissociation.

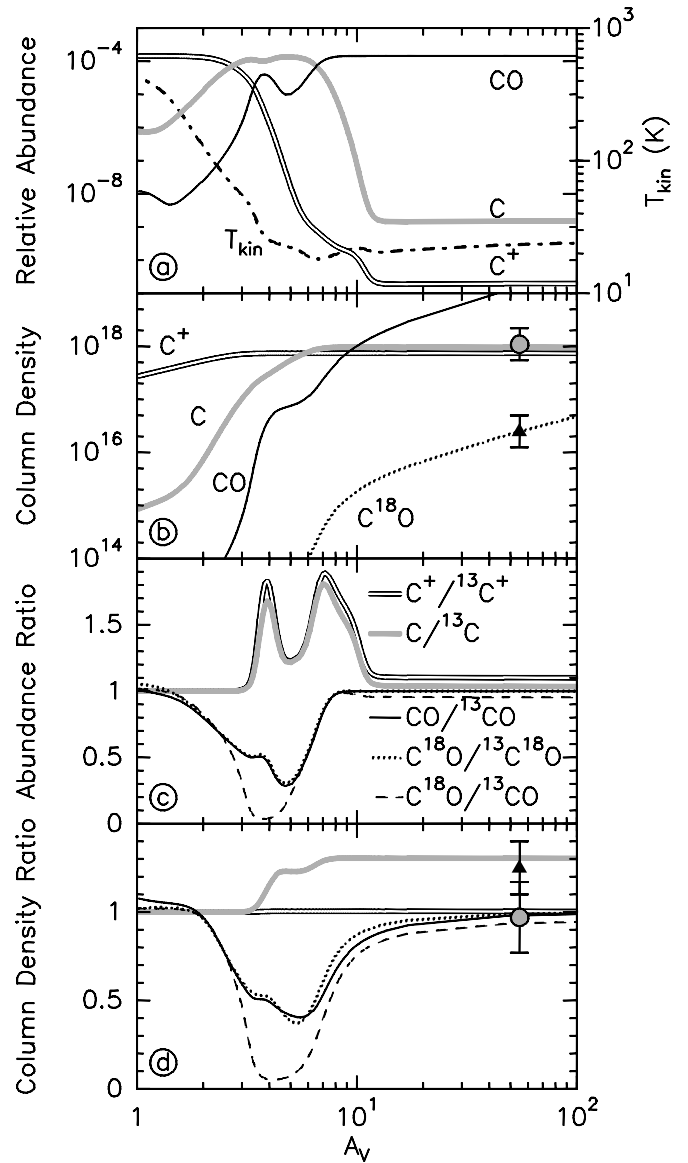


FIG. 2.— Output of the PDR model. *a*) The abundance of the major carbon species as a function of A_V into the cloud. *b*) The column density integrated from the cloud surface to the visual extinction on the A_V axis. The markers show the observed column densities: filled gray circle – $N(\text{C}) = 1.1 \times 10^{18} \text{ cm}^{-2}$, black triangle – $N(\text{C}^{18}\text{O}) = 2.5 \times 10^{16} \text{ cm}^{-2}$. *c*) The local abundance ratio of ^{12}C isotopes or isotopomers to ^{13}C ones, normalized by their input ratios. *d*) The column density ratios integrated from the cloud surface to the visual extinction on the A_V axis with the same key as shown in *c*. The markers show the observed column density ratios: filled gray circle – $N(^{12}\text{C})/60 N(^{13}\text{C}) = 0.97$, black triangle – $N(\text{C}^{18}\text{O})/60 N(^{13}\text{C}^{18}\text{O}) = 1.25$.

their support, Richard Chamberlin and Maryvonne Gerin for help in the observations, Jacques Le Bourlot for help with the PDR model, Bill Langer and

Ewine van Dishoeck for reading and commenting on the manuscript, and Henrik Klein and Frank Lewen for sharing their data before publication.

REFERENCES

- Boreiko, R. T., & Betz, A. L. 1996, *ApJ*, 467, L113
 Centuri n, M., C ssola, C., & Vladilo, G. 1995, *A&A*, 302, 243
 Cooksy, A. L., Saykally, R. J., Brown, J. M., & Evenson, K. M. 1986, *ApJ*, 309, 828
 Flower, D. R., Pineau des F ret, G., & Walmsley, C. M. 1995, *A&A*, 294, 815
 Klein H., Lewen, F., Schieder, R., Stutzki, J., & Winnewisser, G. 1997, *ApJ*, submitted
 Kooi, J. W., Pety, J., Bumble, B., Walker, C. K., LeDuc, H. G., Schaffer, P. L., & Phillips, T. G. 1997, *IEEE Trans MTT*, in press
 Langer, W.D., Graedel, T. E., Frerking, M. A., & Armentrout, P. B. 1984, *ApJ*, 277, 581
 Langer, W.D., & Penzias, A. A. 1990, *ApJ*, 357, 477 (LP90)
 Langer, W.D., & Penzias, A. A. 1993, *ApJ*, 408, 539 (LP93)
 Le Bourlot, J., Pineau des F rets, G., Roueff, E., & Flower, D. R. 1993, *A&A*, 267, 233
 Lis, D. C., Schilke, P., & Keene, J. 1997, *CO: Twenty-five Years of Millimeter-wave Spectroscopy*, W. B. Latter, et al., Kluwer: Dordrecht, 128
 Saykally, R. J., & Evenson, K. E. 1980, *ApJ*, 238, L107
 Tauber, J., Lis, D. C., Keene, J., Schilke, P., & B ttgenbach, T. H. 1995, *A&A*, 297, 567
 Tauber, J. A., Tielens, A. G. G. M., Meixner, M., Goldsmith, P. F. 1994, *ApJ*, 422, 136
 van Dishoeck, E. F., & Black, J. H. 1988, *ApJ*, 334, 771
 Watson, W. D., Anicich, V. G., & Huntress, W. T., Jr. 1976, *ApJ*, 205, L165
 Wilson, T. L., & Rood, R. T. 1994, *ARAA*, 32m 191
 Winnewisser, M., Winnewisser, B. P., & Winnewisser, G. 1985, *Molecular Astrophysics*, G.H.F. Dierksen, W.F. Heubner, & P.W. Langhoff, Dordrecht: Reidel, 375
 Wouterloot, J. G. A., & Brand, J. 1996, *A&AS*, 119, 439
 Yamamoto, S., & Saito, S. 1991, *ApJ*, 370, L103